

Received March 23, 2021, accepted April 12, 2021, date of publication April 29, 2021, date of current version May 6, 2021.

Digital Object Identifier 10.1109/ACCESS.2021.3076668

# Expanded Neo-Fuzzy Adaptive Decayed Brain Emotional Learning Network for Online Time Series Predication

HOUSSEN SALH ALI MILAD<sup>1</sup>, (Member, IEEE), AND JASON GU<sup>1</sup>, (Senior Member, IEEE)

Department of Electrical and Computer Engineering, Dalhousie University, Halifax, NS B3H 4R2, Canada

Corresponding author: Houssem Salh Ali Milad (houssem.milad@dal.ca)

This work was supported by the National Science and Engineering Research Council Canada (NSERC).

**ABSTRACT** The Neo-Fuzzy integrated Adaptive Decayed Brain Emotional Learning (NF-ADBEL) network has recently been proposed for online time series predicting problems. The NF-ADBEL network is suitable for online time series prediction with shorter update intervals and offers features such as fast learning, accuracy, simplicity, and lower computational complexity. However, the neo-fuzzy neuron network in NF-ADBEL was integrated only in the orbitofrontal cortex (OFC) part of the ADBEL network. This paper aims to further improve the performance of the NF-ADBEL network by integrating the neo-fuzzy neuron network into the amygdala (AMY) section as well, inspired by a fully integrated version of a neo-fuzzy-based pattern recognizer. As is known, the AMY has two outputs: one response is based on imprecise information received from the thalamus, and the second response is based on information received from the sensory cortex. In this study, the imprecise response generation is operated as previously, while the other AMY process is treated by neo-fuzzy neurons. The resultant network is called Expanded Neo-Fuzzy integrated Adaptive Decayed Brain Emotional Learning (ENF-ADBEL). The modified network is still simple and meets the requirement for online prediction problems. A few chaotic and stochastic nonlinear systems, namely the Mackey-Glass, Lorenz, Rossler, disturbance storm time index, Narendra dynamic plant identification, wind speed and wind power series, are used to evaluate the performance of the proposed network in terms of the root mean squared error (RMSE) and correlation coefficient (COR) criteria in a MATLAB programming environment.

**INDEX TERMS** Amygdala, brain emotional decayed learning, chaotic time series, disturbance storm time index, dynamic plant identification, forecasting, MATLAB, neo-fuzzy networks, wind speed, wind power series.

## I. INTRODUCTION

A number of different techniques have been applied to the chaotic times series prediction problem, with varying degrees of success. The Artificial Neural Network (ANN) is probably the technique most frequently used. However, due to its structure and back-propagation training algorithm, there is no guarantee that the training processes will not land in a local minima position. Furthermore, there is an increase in time computational complexity with this approach because there is no optimal structure for the number of neurons and number of layers, or for the activation function suitable for the

objective function. These drawbacks affect the reliability and accuracy of the prediction.

The Brain Emotional Learning Neural Network (BELNN) has recently emerged as an alternative to classical artificial neural networks for approximating nonlinear functions. BELNN is inspired by both feed-forward neural networks and fast learning and has been applied to time series prediction techniques [1]–[3].

Several studies [4], [5] have concluded that, in terms of fear conditioning, the limbic system (LS) is primarily responsible for the process of learning emotions, as shown in Fig. 1. Emotions are highly contingent on this area of the brain, so the thalamus (TH) is considered not only a gateway to the LS, but also the means for providing the LS with all available and received information in the form of emotional stimuli [6].

The associate editor coordinating the review of this manuscript and approving it for publication was Shuihua Wang<sup>1</sup>.

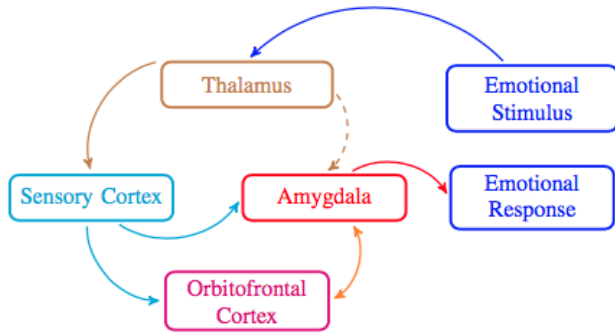


FIGURE 1. Routes of limbic system.

The TH sends the received information along a short path to the amygdala (AMY) and then directly to the sensory cortex (SC). The SC forwards the received information to the AMY and orbitofrontal cortex (OFC).

One of the most important characteristics of the AMY’s emotional learning is that it is permanent and monotonic [7]. The OFC has a mono-direction connection with the SC and a bi-directional relationship with the AMY. Its functions are processing stimuli, analyzing emotional stimuli, and evaluating reinforcement signals and emotional learning to prevent an inappropriate response from the AMY.

A Neo-Fuzzy Adaptive Decayed Brain Emotional Learning (NF-ADBEL) network has recently been proposed in the literature for online time-series prediction problems [2]. The present work aims to investigate and further enhance the performance of the NF-ADBEL network by the addition of a neo-fuzzy neuron network into the AMY section. As is known, the AMY has two outputs: one is based on imprecise information received from the TH, and the other is based on information received from the SC. Here, the imprecise response generation is operated as previously, while the other AMY process is treated by neo-fuzzy neurons. The resultant network, called Expanded Neo-Fuzzy Adaptive Decayed Brain Emotional Learning (ENF-ADBEL), is inspired by a fully integrated version of a neo-fuzzy-based pattern recognizer [8].

To the best of the author’s knowledge, no such integration model has yet been explored in the literature. The proposed ENF-ADBEL network is simulated in a MATLAB (R214a) programming environment to forecast a number of chaotic time series and stochastic problems in an online mode, including Mackey-Glass, Lorenz, Rossler, Narendra, disturbance storm time index, wind speed and wind power series. Comparing the prediction performance of the proposed ENF-ADBEL to NF-ADBEL, F-ADBEL, MLP, and other predictor networks in terms of RMSE and correlation coefficient criteria reveals the superiority of the proposed ENF-ADBEL network in online forecasting problems.

This paper is organized as follows: the proposed network is described in section II, the results and discussion are presented in section III, followed by the conclusions in section IV.

## II. PROPOSED EXPANDED NEO-FUZZY ADAPTIVE DECAYED BRAIN EMOTIONAL LEARNING NETWORK

### A. REVIEW OF ADAPTIVE DECAYED BRAIN EMOTIONAL LEARNING NETWORK

As mentioned in [2], the ADBEL network has four inputs as given by (1) and one output as given by (2). This mapping can be formulated as:

$$P = (p_1 \quad p_2 \quad \dots \quad p_j)^T \quad (1)$$

Here, index ‘j’ refers to the number of past inputs to the network.

$$\hat{P}_t = f(P) \quad (2)$$

After the inputs are presented to the network, the TH computes the presented stimulus’s maximum value (input data) and sends it along a shorter path to the AMY. At the same time, the TH dispatches the presented data to the SC, which sends the information to the AMY and OFC for response generation, as shown in Fig. 1.

Let ‘V’ and ‘W’ be the row vectors containing the AMY and OFC weights, respectively. The response to the stimuli is modelled as follows:

$$V = (v_1 \quad v_2 \quad \dots \quad v_j) \quad (3)$$

$$W = (w_1 \quad w_2 \quad \dots \quad w_j) \quad \forall j = 1, 2, \dots, 4 \quad (4)$$

The AMY produces two outputs,  $E_{AMY}$  and  $\acute{E}_a$ , as:

$$\acute{E}_a = V \times P \quad (5)$$

$$m = \max_j \times P \quad (6)$$

$$E_{AMY} = \acute{E}_a + V_{th} \times m \quad (7)$$

Similarly, the OFC produces one output,  $E_{OFC}$ , as:

$$E_{OFC} = W \times P \quad (8)$$

ADBEL’s output is given by:

$$\hat{P}_t = E_{AMY} - E_{OFC} \quad (9)$$

The steps shown in (7)-(9) are termed prediction steps in [1]. After the prediction stage, the ADBEL network is trained with the help of signals  $E_{AMY}$ ,  $\acute{E}_a$ ,  $E_{OFC}$ ,  $p_t$ , and the constant parameters  $\alpha$ ,  $\beta$ ,  $\gamma$ . The output from the AMY  $E_a$  in combination with the current time series value  $p_t = target (T_t)$  and decay rate  $\gamma$  is used to adjust the AMY weights in the following way:

$$\begin{cases} V(t+1) = (1 - \gamma)V(t) + \alpha \max(T_t - E_{AMY}, 0)P^T \\ V_{th}(t+1) = (1 - \gamma)V_{th}(t) + \alpha \max(T_t - E_{AMY}, 0)m, \end{cases} \quad (10)$$

Firstly, to adjust the weights of the OFC, an internal reward signal  $R_o$  is computed as:

$$R_o = \begin{cases} \max(\acute{E}_a - T_t, 0) - E_{OFC}, & \text{if } (T_t \neq 0) \\ \max(\acute{E}_a - E_{OFC}, 0), & \text{otherwise} \end{cases} \quad (11)$$

Based on this reward signal, the weights of the OFC are updated as:

$$W(t + 1) = W(t) + \beta \times R_o \times P^T \quad (12)$$

### B. REVIEW OF NEO-FUZZY NETWORK

A neo-fuzzy network is a nonlinear learning system. The architecture of a neo-fuzzy neuron with multi-inputs and one output is used in this work, as explained in [2].

### C. EXPANDED NEO FUZZY ADAPTIVE DECAYED BRAIN EMOTIONAL LEARNING NETWORK

Motivated by ADBEL and the common features of neo-fuzzy networks, this work considers a hybrid model called expanded neo-fuzzy adaptive decayed brain emotion learning (ENF-ADBEL) network to improve the further forecasting accuracy of the NF-ADBEL network [2]. In this proposed network, the neo-fuzzy neurons are integrated to the orbitofrontal OFC section and partially in the AMY section, as shown in Fig. 2.

The AMY has two outputs, one of which is related to imprecise information (the maximum value of input data) received from the TH. This part of the network is kept free from neo-fuzzy neurons, while the other part of the AMY network is loaded with neo fuzzy neurons. Note that this modification will not compromise the BEL network's fast-processing feature, i.e., the hybrid network; it can still be used in online mode for time-series prediction. Thus, we have replaced the OFC and AMY weights with neo-fuzzy neurons network weights, except the weight named  $v_{th}$  in the AMY part. The reason for this modification is to add an extra degree to the AMY part in order to help the AMY in a more involved analysis of stimuli received from the SC section, while simultaneously keeping the imprecise information received from the TH.

This approach is inline with the computational model of the limbic system. Collectively, neo-fuzzy neurons are used in the entire OFC section and partially in the AMY section of the ADBEL model. The resulting network is named ENF-ADBEL, as shown in Fig. 2. The working principle of the proposed network remains the same as that of the ADBEL network, but the definition of weight entries and the application of those entries in the learning rules of the AMY and OFC sections are different. The output of the OFC as well as the weights of the neo-fuzzy neurons in the OFC section ( $w_{ij}$ ), along with the corresponding degrees of membership functions ( $h_{ij}$ ), are represented as:

$$E_{OFC,enf} = W_{ij} \times H_{ij} \quad (13)$$

$$W_{ij} = (w_{11} \ w_{12} \ w_{13} \ w_{21} \ w_{22} \ \dots \ w_{ij}) \quad (14)$$

$$H_{ij} = (h_{11} \ h_{12} \ h_{13} \ h_{21} \ h_{22} \ \dots \ h_{ij})^T \quad (15)$$

Similarly, in the ENF-ADBEL network, the AMY output with a different set of neo-fuzzy weights ( $v_{ij}$ ) and corresponding degrees of membership functions ( $h_{ij}$ ) is

determined as:

$$\acute{E}_a = V_{ij} \times H_{ij} \quad (16)$$

$$E_{AMY,enf} = \acute{E}_a + V_{th} \times m \quad (17)$$

$$V_{ij} = (v_{11} \ v_{12} \ v_{13} \ v_{21} \ v_{22} \ v_{23} \ \dots \ v_{ij}) \quad (18)$$

which then leads to:

$$P_{enf}^{\hat{}} = E_{AMY,enf} - E_{OFC,enf} \quad (19)$$

The minimization of the quadratic error function in [2] through the gradient descent method yields the new following parameter adjustment rules:

$$W_{ij}(t + 1) = W_{ij}(t) + \beta(P_{enf}^{\hat{}}(t) - T(t))H_{ij}^T(x_i) \quad (20)$$

$$V_{ij}(t + 1) = \{(1 - \gamma)V_{ij}(t) + \alpha \max(T(t) - E_{AMY,enf}(t), 0) \times H_{ij}^T(x_i)\} \quad (21)$$

$$V_{th}(t + 1) = \{(1 - \gamma)V_{th}(t) + \alpha \max(T(t) - E_{AMY,enf}(t), 0)m\} \quad (22)$$

The learning parameters  $\alpha$ ,  $\beta$  and  $\gamma$  are positive constants and are defined as the learning rates of the neo-fuzzy network. The proposed model mimics emotional learning by integrating a neo-fuzzy neuron. The gradient descent (GD) method is employed for the learning algorithm of the proposed model, which aims to enhance the prediction accuracy in existing computational models that use brain emotional learning processing.

The ENF-ADBEL network's functioning is similar to that of the NF-ADBEL and ADBEL networks. The neo-fuzzy neurons for the ENF-ADBEL network are realized with three triangular membership functions, and the universe of discourse is selected to be [0, 1] as in [2]. Thus, the output of the proposed integrated ENF-ADBEL network is given as:

$$\hat{P}_t = \sum_{j=1}^4 \sum_{k=1}^3 (V_{jk} \times H_{jk} - W_{jk} \times H_{jk}) + V_{th} \times m \quad (23)$$

The unknown weights of the amygdala and orbitofrontal cortex in (23) are adjusted online. **Please note that the proposed ENF-ADBEL network does not have any knowledge about the time series, as is the case with the NF-ADBEL and ADBEL networks.** Previous works on neo-fuzzy networks and state-of-the-art consider training the network with the time series data and then deploying the trained network to do future predictions [9] and [10]. **However, in this work, no prior training of the neo-fuzzy network is assumed.**

### III. RESULTS AND DISCUSSIONS

The proposed ENF-ADBEL network is tested in a MATLAB (R2014a) programming environment for online forecasting of chaotic time-series, including Mackey-Glass, Lorenz, Rossler, Narendra plant, disturbance storm time index, wind speed, and wind power. The performance of the proposed model is accessed in terms of root mean squared error and

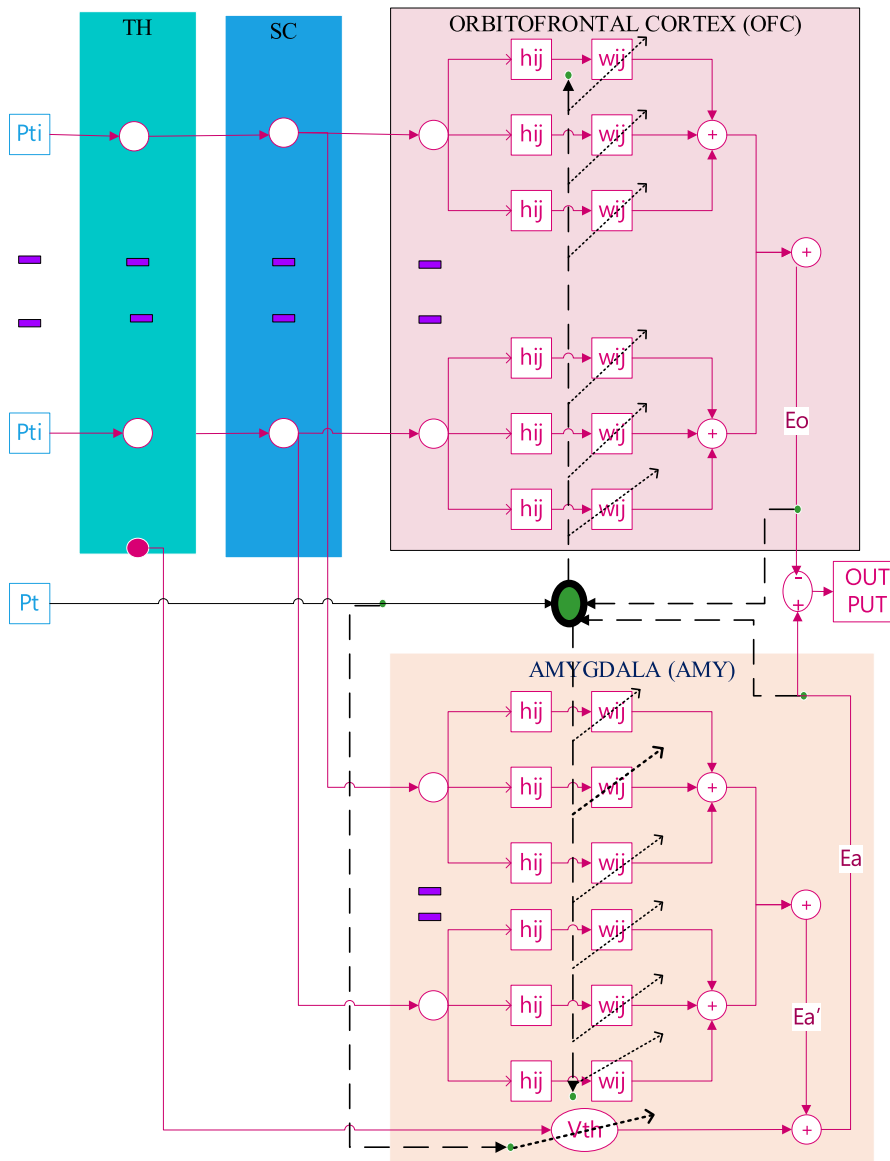


FIGURE 2. Expanded Neo-Fuzzy Adaptive Decayed Brain Emotional Learning Network (ENF-ADBEL).

correlation coefficient criteria. A comparison is also made with NF-ADBEL and F-ADBEL and MLP networks driven by the near-optimal set of alpha, beta and gamma parameters.

A comparison of the proposed model with trained state-of-the-art predictors is drawn against the following performance metrics:

$$RMSE_m = \sqrt{\frac{1}{n_e - n_s} \sum_{i=n_s}^{n_e} e_{mi}^2} \tag{24}$$

$$R_m^2 = \frac{\sum_{i=n_s}^{n_e} (\hat{P}_{mti} - \bar{\hat{P}}_{mt})(P_{ti} - \bar{P}_t)}{\sqrt{\sum_{i=n_s}^{n_e} (\hat{P}_{mti} - \bar{\hat{P}}_{mt})^2} \sqrt{\sum_{i=n_s}^{n_e} (P_{ti} - \bar{P}_t)^2}} \tag{25}$$

$$PI = \frac{PC_{m_1} - PC_{m_2}}{PC_{m_1}} \times 100 \tag{26}$$

subscript..(m) can be ( $m_1$ ) denoting:

- NF – ADBEL, F – ADBEL,
- MLP, ..etc
- or( $m_2$ )representingENF – ADBEL
- $n_e$  = numberofsamples
- $n_s$  = steadystatestarts
- $i = n_s$
- $R_m^2$  = correlationcoefficient,
- $m^{th}$  = networkused
- $\hat{P}_{mti}$  = predictedvaluewith $m^{th}$ network
- $\bar{\hat{P}}_{mt}$  = meanpredictedvaluewith $m^{th}$ network
- $P_{ti}$  = t arg etvalue
- $\bar{P}_t$  = meanoft arg etvalue
- PI = percentageimprovementrespectto =  $m_1$

The time series data are first normalized to the range [0, 1] to run the simulations. The normalized data are then organized so that the first four samples form the inputs, while the fifth sample includes the output. We used the same technique as in [2].

**A. MACKEY-GLASS TIME SERIES AS PREDICTED BY ENF-ADBEL NETWORK**

The Mackey-Glass system is presented as a model of white blood cell production [11]. Let us first predict the time series data generated from a time-delayed Mackey-Glass nonlinear differential equation, which has been used as a benchmark by the researchers for validating their prediction algorithms [12], [13]. The series can be defined as mentioned in [2].

A total of  $n_e = 1200$  data points are generated for testing the networks. By setting the learning parameters to be  $\alpha = 0.5$ ,  $\beta = 0.5$  and  $\gamma = 0.07$ , an ENF-ADBEL network is first deployed to predict the time series.

The same time series is also predicted with NF-ADBEL and F-ADBEL networks using the learning parameters:  $\alpha = 0.5$ ,  $\beta = 0.2$ , and  $\gamma = 0.03$ , while in the case of F-ADBEL the parameters vary. The prediction errors are recorded in all the networks, with analysis showing that the transient period remains the same:  $\leq 5$  s. Thus, the steady-state starting index is set to  $e_s = 5$  sec in all the networks to compute the performance indices.

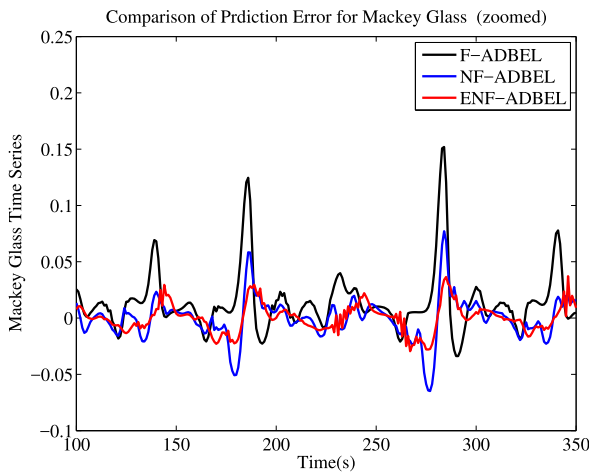


**FIGURE 3. Error comparison for Mackey-Glass time series as predicted by F-ADBEL, NF-ADBEL and ENF-ADBEL networks.**

As can be seen in Fig. 3, the ENF-ADBEL network has performed better than the F-ADBEL and NF-ADBEL networks, showing lower peaks in the prediction error. Further, the root mean squared error and correlation coefficient are also determined for all the networks using the relations in (24) and (25). The computed values are shown in Table 1.

A lower root mean squared error of the ENF-ADBEL network offers less squared error and a higher correlation coefficient for predicting the Mackey-Glass time series compared to F-ADBEL and NF-ADBEL networks. A significant amount of percentage improvement is also obtained,

**TABLE 1. RMSE &  $R^2$  for Mackey-Glass time series prediction by ENF-ADBEL, NF-ADBEL, and F-ADBEL networks.**

TS	Prediction Network	RMSE	$R^2(\%)$	PI(%)
M-G	ENF-ADBEL	0.011	99.89	38.88 & 67.26
	NF-ADBEL [2]	0.018	99.71	
	F-ADBEL	0.0336	99.39	

as expressed in (26). Please note that the results in Table 1 are obtained by the proposed network where no prior training data is assumed.

The authors in [14] proposed a short-term prediction of a backpropagation network (BP) based on the difference method (DMBP). BP is a popular neural network that is widely used for prediction. The structure of the BP network is a multilayer feed-forward network, trained according to error backpropagation. DMBP structures the training layer as two sub-layers, with the change degree layer reflecting the absolute value. Note that the change trend layer reflects by positive and negative data to overcome prediction error. The DMBP method is applied to the Mackey-Glass time series and the results compared to other methods such as BP, support vector regression machine (SVR), and autoregressive integrated moving average (ARIMA) in terms of RMSE. The authors in [14] use 70% of the data as training data and 30% as test data. The results for DMBP in [14] are shown in Table 2.

**TABLE 2. RMSE &  $R^2$  for Mackey-Glass time series prediction by ENF-ADBEL, BP, SVR, NARIMA, and DMBP networks.**

TS	Prediction Network	RMSE	$R^2(\%)$	PI(%)
M-G	ENF-ADBEL	0.0094	99.87	improved by
	DMBP [14]	0.041	-	77.07
	NARIMA [14]	0.05	-	81.20
	SVR [14]	0.23	-	95.91
	BP [14]	0.291	-	96.76

To obtain a fair comparison of the presented network with the methods in [14], the ENF-ADBEL proposed network readjusted the learning parameters to  $\alpha = 0.54$ ,  $\beta = 0.5$  and  $\gamma = 0.07$ , and the steady-state was selected as 50 seconds, which reflects 4% of the data points. The results presented in Table 2 show that the proposed ENF-ADBEL network had a better performance in RMSE. Specifically, it recorded a running time of 0.18 seconds, reflecting its simplicity and fast learning. It thus can be deployed for online prediction.

Furthermore, a multilayer perceptron (MLP) neural network is used for the same Mackey-Glass data points to compare the proposed ENF-ADBEL. According to [15], MLP is the most popular neural network for time series data forecasting. In MLP, we structured the network for ten hidden layers and used the GD method, and the data were divided 70% as trained data, 15% as validated data, and 15% as tested data. The results presented in Table 3 show how ENF-ADBEL's performance was significantly improved and gave better outcomes.



**TABLE 3. RMSE &  $R^2$  for Mackey-Glass time series prediction by ENF-ADBEL and MLP networks.**

Time Series	Prediction Network	RMSE	$R^2$ (%)	PI(%)
Mackey-Glass	ENF-ADBEL	0.011	99.89	66.66
	MLP	0.033	98.28	

### B. LORENZ TIME SERIES AS PREDICTED BY ENF-ADBEL NETWORK

The Lorenz system was presented in 1963 by Lorenz in [16]. We simulated the ENF-ADBEL to predict the x-dynamics of the Lorenz chaotic time series. This series has also been used in various studies to verify the performance of prediction algorithms [17]- [18]. The series is generated by [16] from the coupled differential equations; for more details, refer to [2].

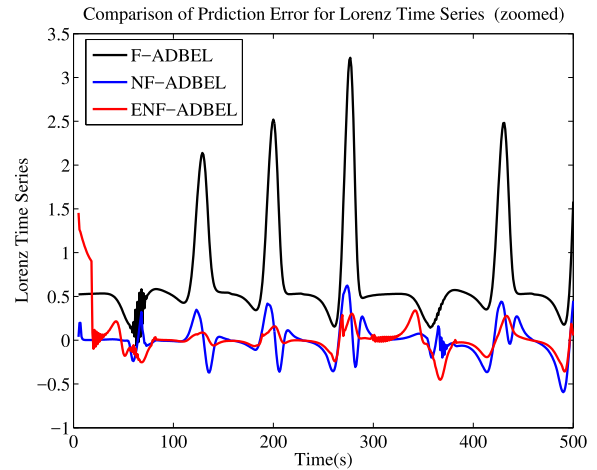
For the generated Lorenz time series with  $n_e = 16380$ , we first evaluate the prediction performance of the ENF-ADBEL network, with the learning parameters set as  $\alpha = 0.5$ ,  $\beta = 0.3$ , and  $\gamma = 0.04$ .

It was found that the prediction results of the ENF-ADBEL network for the Lorenz time series performs better when compared to results for the Mackey-Glass time series. Specifically, it is difficult to distinguish the predicted Lorenz time series from the target data. The running time for the proposed network was 1.47 seconds. For comparison purposes, we simulated the NF-ADBEL and F-ADBEL networks to predict the Lorenz time series. We found the best learning parameters for the NF-ADBEL network in predicting the Lorenz time series to be  $\alpha = 0.8$ ,  $\beta = 0.2$ , and  $\gamma = 0.01$ , while for F-ADBEL the parameters varied; the running time was found to be 1.42 and 20.50 seconds, respectively. By recording and analyzing the prediction error in all cases, it was found that the transient period is less than 5s, and therefore the steady-state starting index is taken as  $n_s = 5$ .

**TABLE 4. RMSE &  $R^2$  for Lorenz time series as predicted by ENF-ADBEL, NF-ADBEL, and F-ADBEL networks.**

TS	Prediction Network	RMSE	$R^2$ (%)	PI(%)
Lorenz	ENF-ADBEL	0.13054	99.98	24.36 & 84.75
	NF-ADBEL [2]	0.1726	99.97	
	F-ADBEL	0.8564	99.78	

A zoomed view of the prediction error as returned by all networks in steady-state is shown in Fig. 4. The figure shows that the proposed ENF-ADBEL network has a lower error in predicting the Lorenz time series compared to the existing NF-ADBEL and F-ADBEL networks. The prediction performance in all cases is also analyzed in terms of root mean squared error in (24), as shown in Fig. 4, and in terms of the correlation coefficient criterion (25). The results for this analysis are included in Table 4. As can be seen, superior performance is provided by the ENF-ADBEL network due to the lower root mean squared error, higher correlation coefficient, and significant percentage improvement offered by this network.

**FIGURE 4. Error comparison in Lorenz time series as predicted by F-ADBEL, NF-ADBEL and ENF-ADBEL networks.**

The authors in [10] used a long-short-term-memory (LSTM) recurrent neural network to predict the Lorenz time series. However, the LSTM recurrent network had difficulty representing temporal and non-temporal inputs simultaneously in multivariate data. In [10], the authors proposed a hierarchical decomposition of univariate LSTMs and combined the resulting features in final feed-forward layers. The model was selected based on early stopping, with 20% validation data of the 3,000 data samples used over 1,000 epochs. The condition was: If the validation performance is not improved within 100 epochs, then training is stopped. The authors in [10] applied the proposed LSTM to the Lorenz time series and compared one-step-ahead prediction error in terms of lowest RMSE and high correlation coefficient to other approaches such as Naïve LSTM and multivariate interpolated LSTM. The LSTM approach gave better results compared to the other methods.

For fair comparison to the ENF-ADBEL network, we used 75% data as a steady-state. The parameters of ENF-ADBEL were tuned as  $\alpha = 0.49$ ,  $\beta = 0.42$ , and  $\gamma = 0.04$ . The proposed ENF-ADBEL showed better results in low prediction error and high correlation, as presented in Table 5. According to [10], the used LSTM converged within several hours of training, while the proposed ENF-ADBEL performed convergence within a few seconds. The running time was 1.44 seconds, showing the best performance and fastest response.

We then applied a multilayer perceptron (MLP) neural network to the same Lorenz data to validate the proposed ENF-ADBEL. The comparison results are given in Table 6, showing that the ENF-ADBEL network performed with better accuracy.

### C. ROSSLER TIME SERIES AS PREDICTED BY ENF-ADBEL NETWORK

We deployed the ENF-ADBEL network to predict the Rossler chaotic time series, as it has been used in the literature to evaluate the performance of prediction algorithms [19]. The time

**TABLE 5. RMSE &  $R^2$  for Lorenz time series prediction by ENF-ADBEL, Naive LSTM, multivariate interpolated LSMT, and LSTM approach networks.**

Time Series	Prediction Network	RMSE	$R^2(\%)$	PI(%)
Lorenz	ENF-ADBEL	0.0217	99.97	improved by
	LSTM approach [10]	0.0282	99.57	23.04
	Multivariate interpolated LSTM [10]	0.0365	99.06	40.54
	Naive LSTM [10]	0.0463	98.89	53.13

**TABLE 6. RMSE &  $R^2$  for Lorenz time series prediction by ENF-ADBEL and MLP networks.**

Time Series	Prediction Network	RMSE	$R^2(\%)$	PI(%)
Lorenz	ENF-ADBEL	0.1305	99.98	69.76
	MLP	0.43	99.96	

series is generated through the differential equations [20], as referred to in [2]. A total of  $n_e = 8188$  samples were generated for the Rossler time series. To simulate the proposed ENF-ADBEL network for predicting this time series, the learning parameters were selected as  $\alpha = 0.5$ ,  $\beta = 0.4$ , and  $\gamma = 0.1$ .

We also simulated the NF-ADBEL network driven by the parameters  $\alpha = 0.5$ ,  $\beta = 0.25$ , and  $\gamma = 0.08$  to forecast the Rossler time series as well as the F-ADBEL network with various parameters. A comparison of all networks in terms of the prediction error is displayed in zoomed view in Fig. 5. The transient period happens to be the same as in the case of the Mackey-Glass and Lorenz time series, i.e.,  $n_s = 5$  s.

**TABLE 7. RMSE &  $R^2$  for Rossler time series prediction by ENF-ADBEL, NF-ADBEL, and F-ADBEL networks.**

TS	Prediction Network	RMSE	$R^2(\%)$	PI(%)
Rossler	ENF-ADBEL	0.2193	99.96	26.87 & 82.45
	NF-ADBEL [2]	0.2999	99.92	
	F-ADBEL	1.2498	99.26	

Furthermore, the amplitude of the error signal for the ENF-ADBEL network is lower compared to the NF-ADBEL and F-ADBEL networks, as shown in Fig. 5. This figure indicates the better prediction accuracy of the ENF-ADBEL network. Analysis of the predicted results for the Rossler time series in terms of the root mean squared error and correlation coefficient criteria are shown in Table 7. As can be seen, the results reveal the superiority of the ENF-ADBEL over the NF-ADBEL and F-ADBEL networks. Finally, a reasonable amount of percentage improvement is yielded by the ENF-ADBEL network for predicting the Rossler time series, as presented in Table 7.

Moreover, we applied an MLP neural network for the same Rossler data to validate the proposed ENF-ADBEL. The comparison results, as shown in Table 8, demonstrate that the ENF-ADBEL network performed with better accuracy.

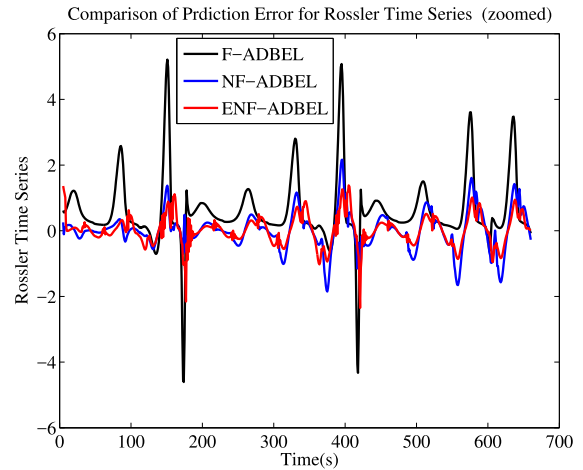


**FIGURE 5. Error comparison in Rossler time series as predicted by F-ADBEL, NF-ADBEL and ENF-ADBEL networks.**

**TABLE 8. RMSE &  $R^2$  for Rossler time series prediction by ENF-ADBEL and MLP networks.**

Time Series	Prediction Network	RMSE	$R^2(\%)$	PI(%)
Rossler	ENF-ADBEL	0.2193	99.96	75.22
	MLP	0.885	99.40	

#### D. DISTURBANCE STORM TIME INDEX PREDICTED BY ENF-ADBEL NETWORK

Precise forecasting of space weather, especially solar storms, has become increasingly urgent because of the destructive effects these storms can have on infrastructures such as satellites, telecommunication, and power grids [7]. Recently, the ADBEL network also proposed predicting this important index [1], along with NF-ADBEL in [2], which has been modified in the present work to yield to the ENF-ADBEL network. Here, we simulated the ENF-ADBEL network to predict the disturbance storm time index  $D_{st}$  time series for the month of April 2000, when considerable geomagnetic activity was observed. The data for this month have been downloaded from the website World Data Center (WDC) [21], “WDC for Geomagnetism, Kyoto.”

With the learning parameters set as  $\alpha = 0.15$ ,  $\beta = 0.38$  and  $\gamma = 0.25$ , the ENF-ADBEL network was deployed to predict the  $D_{st}$  index for the month of April 2000. The number of samples is  $n_e = 716$  for that month.

**TABLE 9. RMSE &  $R^2$  for Dst April 2000 by ENF-ADBEL, NF-ADBEL, and F-ADBEL networks.**

TS	Prediction Network	RMSE	$R^2(\%)$	PI(%)
Dst	ENF-ADBEL	6.86	98.31	24.44 & 47.78
	NF-ADBEL [2]	9.08	97.06	
	F-ADBEL	13.137	94.36	

The predicted results provided by the ENF-ADBEL network are shown in Table 9. The transient period of the ENF-ADBEL network is  $n_s = 10$  hrs, which then becomes the steady-state starting index. It can be observed that, despite

the high initial transients, the ENF-ADBEL network can follow the  $D_{st}$  time series in steady-state. The important valley points are also well-predicted, which points to the possible occurrence of geomagnetic storms.

To draw a comparison, an existing NF-ADBEL network in [2] is used to predict the  $D_{st}$  time series. For this purpose, the learning parameters of the NF-ADBEL network are assigned the values of  $\alpha = 0.3$ ,  $\beta = 0.3$ , and  $\gamma = 0.01$ . This comparison in terms of the prediction error and correlation coefficients showed that the ENF-ADBEL network has better performance than the NF-ADBEL and F-ADBEL networks, as illustrated in Fig. 6 and Table 9.

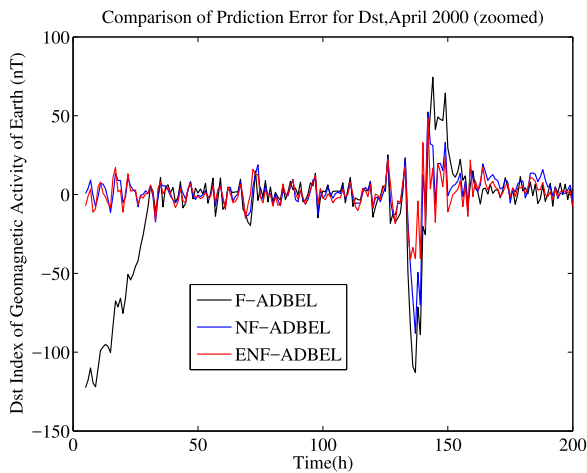


FIGURE 6. Comparison error of disturbance storm time index for April 2000 as predicted by F-ADBEL, NF-ADBEL and ENF-ADBEL networks.

The authors in [9] designed an NFCBEL predictor that combines a type of emotional neural network and neo-fuzzy neurons. The NFCBEL is deployed to predict Dst between 2000 and 2006. After training the NFCBEL offline, 70% and 30% of the data are used for predicting. The performance of RMSE and correlation is shown in Table 10.

TABLE 10. RMSE &  $R^2$  for Dst prediction by ENF-ADBEL and NFCBEL networks.

Time Series	Prediction Network	RMSE	$R^2(\%)$	Epochs
Dst Apr 2000	ENF-ADBEL	4.05	98.07	0
Dst [9]	NFCBEL	4.7649	98.047	50

To make a fair comparison between the proposed model and the model in [9], the proposed ENF-ADBEL is deployed to predict Dst for April 2000 for 28% of 716 data points as  $n_s = 200$ . The ENF-ADBEL network is then assigned the values of  $\alpha = 0.1$ ,  $\beta = 0.3$ , and  $\gamma = 0.93$ . The proposed model performed with good results for RMSE and high correlation, as shown in Table 10. The running time was 0.98 seconds. ENF-ADBEL performed well compared to NFCBEL, which performed its outcomes after 50 iterations. Please note that because the length of the data is not the same,

the results in Table 10 reflect the performance of the proposed model based on available data, in this case, April 2000.

To provide a fairer comparison, an MLP was used to predict Dst for the same data (April 2000). The comparison results are displayed in Table 11. As can be seen, the ENF-ADBEL network performed with better accuracy.

TABLE 11. RMSE &  $R^2$  for Dst for April 2000 prediction by ENF-ADBEL and MLP networks.

TS	Prediction Network	RMSE	$R^2(\%)$	PI(%)
Dst April 2000	ENF-ADBEL	6.86	98.31	7.5
	MLP	7.42	95.32	

### E. NARENDRA DYNAMIC PLANT PREDICTED BY ENF-ADBEL NETWORK

We also simulated the ENF-ADBEL network for the online identification of the Narendra dynamic plant, which was described in [2].

A total of  $n_e = 1996$  samples are used in this work. The ENF-ADBEL network was first deployed to identify the dynamic plant using the learning parameters  $\alpha = 0.4$ ,  $\beta = 0.49$ , and  $\gamma = 0.09$ . As can be seen, the ENF-ADBEL network was able to identify the dynamic plant. The steady-state starting index was taken as  $n_s = 5 \text{ sec}$ . To compare the performance of ENF-ADBEL network to NF-ADBEL and F-ADBEL, the simulation is run with the learning parameters for the NF-ADBEL network set as  $\alpha = 0.3$ ,  $\beta = 0.5$ , and  $\gamma = 0.01$  as in [2]. Varying parameter values were used for the F-ADBEL network. The identification error is presented in Table 12.

TABLE 12. RMSE &  $R^2$  for Narendra identification plant by ENF-ADBEL, NF-ADBEL, and F-ADBEL networks.

TS	Prediction Network	RMSE	$R^2(\%)$	PI(%)
N.Plant	ENF-ADBEL	0.0129	99.99	20.37 & 83.56
	NF-ADBEL [2]	0.0162	99.98	
	F-ADBEL	0.0785	99.87	

The transient period of the NF-ADBEL network is the same as that of the ENF-ADBEL network. However, the ENF-ADBEL network shows better performance compared to the NF-ADBEL and F-ADBEL networks, as illustrated in Fig. 7, owing to the lesser identification error being offered by this network during steady-state. A lower root mean squared error, higher correlation coefficient and sufficient percentage improvement as obtained by the ENF-ADBEL network validates its superior performance over the NF-ADBEL and F-ADBEL networks in identifying the Narendra plant, as presented in Table 12.

We applied an MLP neural network for the same Narendra plant data to validate the proposed ENF-ADBEL. The comparison results are presented in Table 13. The results show that the ENF-ADBEL network performed with significant accuracy.



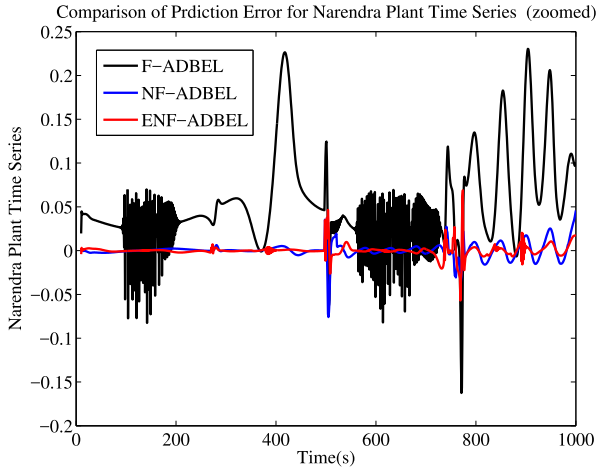


FIGURE 7. Comparison error of Narendra dynamic plant as predicted by F-ADBEL, NF-ADBEL and ENF-ADBEL networks.

TABLE 13. RMSE &  $R^2$  for Narendra plant prediction by ENF-ADBEL and MLP networks.

Time Series	Prediction Network	RMSE	$R^2$ (%)	PI(%)
Narendra Plant	ENF-ADBEL	0.0129	99.99	56.71
	MLP	0.0298	99.94	

F. WIND SPEED PREDICTED BY ENF-ADBEL NETWORK

Conventional methods of generating electricity are continuously polluting the environment. Renewable energy resources have the potential both to overcome the problem of air pollution and to meet the load demand. Among various renewable energy resources, wind energy offers a viable way to harness electricity, owing to its cost-effectiveness and sustainable nature [22]. However, available wind power depends on wind speed.

Due to the randomly fluctuating characteristics of wind speed, the prediction results of wind power may change rapidly. Accurate wind speed prediction can significantly improve power quality, security, supply-demand balancing and, in general, wind generation management in the intelligent grid [23]. Therefore, applying wind speed prediction techniques that offer the best forecasting accuracy over time scales is required [24].

In this paper, a proposed ENF-ADBEL is used to predict wind speed. Hourly wind speed data for three months (January, February and March 2020) are obtained from a Canadian meteorological station located in Lunenburg, Nova Scotia [25], and applied to the proposed network.

To investigate the behaviour of ENF-ADBEL in forecasting wind speed, the network is first employed using the learning parameters  $\alpha = 0.3$ ,  $\beta = 0.015$ , and  $\gamma = 0.25$ . As can be seen, the ENF-ADBEL network can predict wind speed for one hour ahead. The steady-state starting index is taken to be  $n_s = 1hr$ . For comparison purposes, the simulation runs with the learning parameters for the NF-ADBEL network set as  $\alpha = 0.77$ ,  $\beta = 0.04$ , and  $\gamma = 0.19$ , with varying parameters values for the F-ADBEL network. The forecasting errors

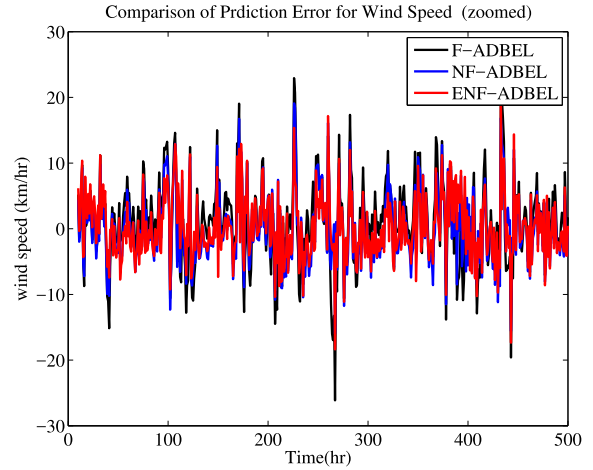


FIGURE 8. Comparison error of wind speed as predicted by F-ADBEL, NF-ADBEL and ENF-ADBEL networks.

TABLE 14. RMSE &  $R^2$  for wind speed ENF-ADBEL, NF-ADBEL, and F-ADBEL networks.

TS	Prediction Network	RMSE	$R^2$ (%)	PI(%)
Wind.S	ENF-ADBEL	5.28	89.08	4.52 & 28.97
	NF-ADBEL	5.53	88.10	
	F-ADBEL	6.81	86.01	

are shown in Fig. 8, and the outcome results are presented in Table 14.

As can be seen, the ENF-ADBEL network gives a better performance than the NF-ADBEL and F-ADBEL networks, owing to fewer forecasting errors by this network during steady-state. In terms of running time, the proposed ENF-ADBEL took 1.09 seconds, NF-ADBEL took 1.03 seconds, and F-ADBEL took 3.7 seconds. A lower root mean squared error, higher correlation coefficient and sufficient percentage improvement as yielded by the ENF-ADBEL network validates its satisfactory performance over the NF-ADBEL and F-ADBEL networks in wind speed prediction, as shown in Table 14.

The authors in [26] built eight models to predict wind speed (BPNN, GA-BPNN, PSO-BPNN, LSTM, SVR, GA-SVR, Bagging and Boosting) supported by GA and PSO to help find a global optimal. They used a dataset from Open EI with a data size of 36,295 samples. The data are from May 13, 2003 to Jan 20, 2004 and are randomly split into a training set and a test set, with 70% of the data for training and 30% for testing. We used the correlation coefficient criteria to compare the results of the different models to the proposed ENF-ADBEL network. The results in Table 15 show that the proposed model has high correlation and fast processing, since the other methods were trained and accomplished the performance within 1,000 iterations. Please note that the data used in the proposed model, in this case, are different in size and location.

We applied an MLP neural network for the same wind speed data to validate the proposed ENF-ADBEL. The comparison results indicate that it performed with fair accuracy, as shown in Table 16.

**TABLE 15.**  $R^2$  for wind speed prediction by ENF-ADBEL, BPNN, GA-BPNN, PSO-BPNN, LSTM, SRV, GA-SVR, bagging, and adaboost models.

Time Series	Prediction Network	$R^2$ (%)
Wind Speed	ENF-ADBEL	98.08
	BPNN [26]	88.76
	GA-BPNN [26]	88.47
	PSO-BPNN [26]	87.21
	LSTM [26]	87.99
	SRV [26]	88.35
	GA-SRV [26]	88.55
	Bgging [26]	88.63
Adaboost [26]	88.55	

**TABLE 16.** RMSE &  $R^2$  for wind speed prediction by ENF-ADBEL and MLP networks.

Time Series	Prediction Network	RMSE	$R^2$ (%)	PI(%)
Wind Speed	ENF-ADBEL	5.28	89.08	2.76
	MLP	5.43	88.81	

**G. WIND POWER PREDICTED BY ENF-ADBEL NETWORK**

In recent decades, immense efforts have been made to develop efficient wind power forecasting models at multiple scales. Accurate wind power forecasting can help to arrange generation plans, maintain grid stability, and provide a reliable basis for grid operation [27]. Different approaches were used for different time scales and data sources [28].

In this work, we used seven-day-ahead hourly wind power data obtained from [29] to apply to the proposed ENF-ADBEL network. These wind power data indicate the amount available to Alberta, Canada, from a grid for a seven-day-ahead basis with energy updates every six hours. The data indicate three expected wind power availability levels: minimum wind power, most-likely available wind power, and maximum wind power forecast.

Firstly, we simulated the proposed ENF-ADBEL network for predicting wind power in terms of minimum wind power data. The learning parameters were  $\alpha = 0.47$ ,  $\beta = 0.32$ , and  $\gamma = 0.14$ . The NF-ADBEL network driven by the parameters  $\alpha = 0.4$ ,  $\beta = 0.5$ , and  $\gamma = 0.13$  was also simulated to forecast minimum wind power, as was the F-ADBEL network with various parameters. The proposed model's outcome in terms of low RMSE and high correlation is presented in Table 17.

**TABLE 17.** RMSE &  $R^2$  for minimum wind power predicted by ENF-ADBEL, NF-ADBEL, F-ADBEL networks.

TS	Prediction Network	RMSE	$R^2$ (%)	PI(%)
Wind.P	ENF-ADBEL	16.28	99.70	15.03 & 63.71
	NF-ADBEL	19.16	99.59	
	F-ADBEL	44.87	98.12	

A comparison of all networks in terms of the prediction error is displayed in Fig. 9. As can be seen, the amplitude of the error signal for the ENF-ADBEL network is lower

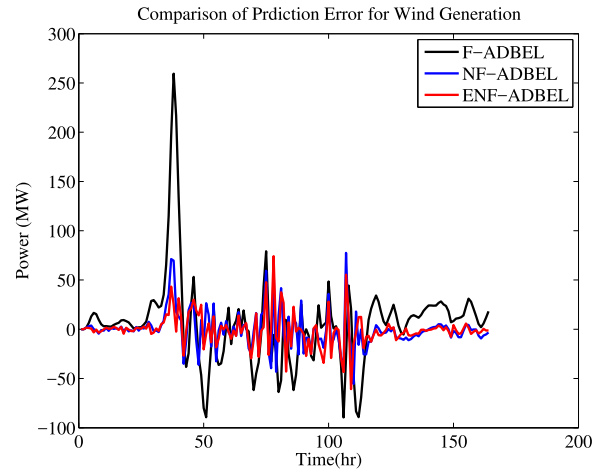


**FIGURE 9.** Comparison error of minimum wind generation as predicted by F-ADBEL, NF-ADBEL and ENF-ADBEL networks.

than for the NF-ADBEL and F-ADBEL networks, with ENF-ADBEL indicating better prediction accuracy. Analysis of predicted results for minimum power forecasting data in terms of RMSE and correlation coefficient criteria is given in Table 17. As shown, ENF-ADBEL gives a better performance than the NF-ADBEL and F-ADBEL networks. Overall, a reasonable amount of percentage improvement is yielded by the ENF-ADBEL network for predicting minimum wind power.

We also applied an MLP neural network for the same wind power data (minimum power) to validate the proposed ENF-ADBEL. The comparison results are given in Table 18, showing that the ENF-ADBEL network performed with better accuracy.

**TABLE 18.** RMSE &  $R^2$  for minimum wind power prediction by ENF-ADBEL and MLP networks.

Time Series	Prediction Network	RMSE	$R^2$ (%)	PI(%)
Min Wind Power	ENF-ADBEL	16.28	99.7	33.95
	MLP	24.65	98.15	

**TABLE 19.** RMSE &  $R^2$  for most likely wind power predicted by ENF-ADBEL, NF-ADBEL, and F-ADBEL networks.

Time Series	Prediction Network	RMSE	$R^2$ (%)	PI(%)
Wind Power	ENF-ADBEL	17.34	99.87	12.82 & 72.13
	NF-ADBEL	19.89	99.83	
	F-ADBEL	62.23	98.81	

Secondly, the proposed ENF-ADBEL network was deployed for predicting the most likely wind power data. The learning parameters were selected as  $\alpha = 0.4$ ,  $\beta = 0.44$ , and  $\gamma = 0.24$ . The NF-ADBEL network, using the parameters  $\alpha = 0.43$ ,  $\beta = 0.49$ , and  $\gamma = 0.13$ , was also simulated to forecast the most-likely wind power, along with the F-ADBEL network, which applied varying parameters. The results in terms of low root mean square error and high correlation are given in Table 19.

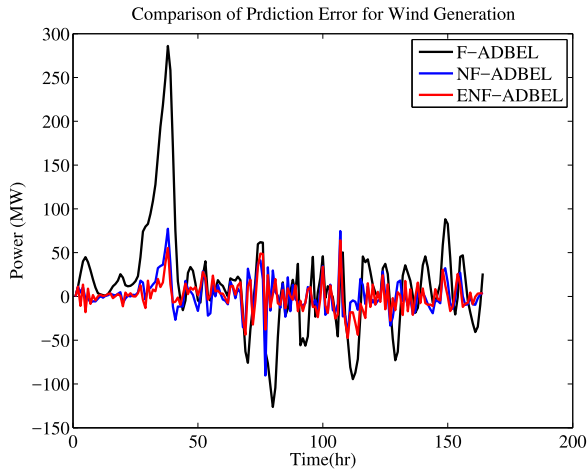


FIGURE 10. Comparison error of most-likely wind generation as predicted by F-ADBEL, NF-ADBEL and ENF-ADBEL networks.

A comparison of all networks in terms of the prediction error is displayed in Fig.10. As can be seen, the amplitude of the error signal for the ENF-ADBEL network is lower compared to the NF-ADBEL and F-ADBEL, which have considerable fluctuation. This shows the better performance accuracy of the ENF-ADBEL network. Analysis of the predicted results for most-likely power forecasting data in terms of the RMSE and correlation coefficient criteria are presented in Table 19. As can be seen, ENF-ADBEL has better results than the NF-ADBEL and F-ADBEL networks, with ENF-ADBEL showing a fair amount of percentage improvement for predicting most-likely wind power.

TABLE 20. RMSE & R<sup>2</sup> for most-likely wind power prediction by ENF-ADBEL and MLP networks.

TS	Prediction Network	RMSE	R <sup>2</sup> (%)	PI(%)
Most Wind.P	ENF-ADBEL	17.34	99.87	44.51
	MLP	31.25	99.79	

The comparison error for the most-likely wind power MLP neural network was used for the same wind power data (most-likely power) to validate the proposed ENF-ADBEL. The comparison results are given in Table 20. The results indicate that the ENF-ADBEL network performed wind generation prediction with better accuracy than the F-ADBEL, NF-ADBEL and ENF-ADBEL networks.

Finally, the proposed ENF-ADBEL network was arranged for predicting maximum wind power data. The learning parameters were selected as  $\alpha = 0.23$ ,  $\beta = 0.45$ , and  $\gamma = 0.09$ . The NF-ADBEL network, using the parameters  $\alpha = 0.2$ ,  $\beta = 0.5$ , and  $\gamma = 0.18$ , was also simulated to forecast maximum wind power, as well as F-ADBEL network, the latter with varying parameters. The results in terms of low root mean square error and high correlation are given in Table 21.

A comparison of all networks in terms of the prediction error is displayed in Fig. 11. As can be seen, the

TABLE 21. RMSE & R<sup>2</sup> for max wind power ENF-ADBEL, NF-ADBEL, and F-ADBEL networks.

TS	Prediction Network	RMSE	R <sup>2</sup> (%)	PI(%)
Wind.P	ENF-ADBEL	29.75	99.78	0.53 & 60.26
	NF-ADBEL	29.91	99.78	
	F-ADBEL	74.88	99.09	

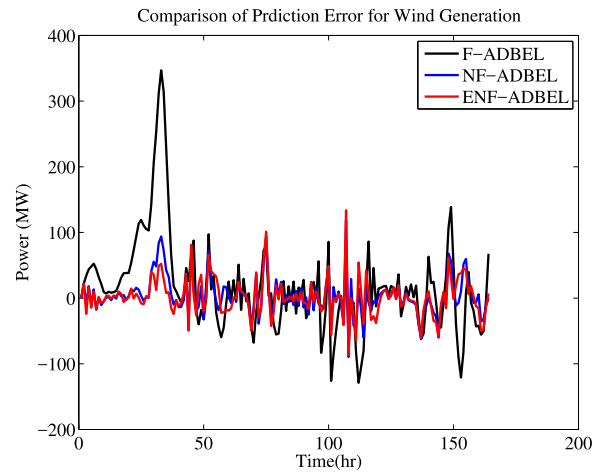


FIGURE 11. Comparison error for max wind generation as predicted by F-ADBEL, NF-ADBEL and ENF-ADBEL networks.

amplitude of the error signal for the ENF-ADBEL network is lower compared to the NF-ADBEL and F-ADBEL networks, which have considerable variation. Therefore, the ENF-ADBEL network presented a remarkable and fair performance accuracy.

Additionally, analysis of the predicted results for maximum power forecasting data in terms of the RMSE and correlation coefficient criteria is presented in Table 21. As shown, the ENF-ADBEL network gives a better performance than the NF-ADBEL or F-ADBEL network. Finally, a fair amount of percentage improvement is yielded by the ENF-ADBEL network for predicting maximum wind power. The proposed ENF-ADBEL network illustrates the best fitting ability for multiple wind power series among all the implemented networks.

The authors in [30] used a hybrid model for short-term wind power forecasting. This model includes vibrational mode decomposition (VMD), the K-means culturing algorithm, and a long-short-term memory (LSTM) network. The model used in [30] evaluated and compared seven different models, including the backpropagation neural network BPNN, the Elman neural network ELMAN, LSTM, VMD-MP, VMD-LSTM, and VMD-K-means-LSTM. The models were applied to forecasting four wind power series for multiple scales. The data utilized in [30] were obtained from the last quarter of 2012 and the first quarter of 2013, while the data used for wind power forecasting were divided as 80% for training data and 20% for testing data.

Table 22 presents the results of methods in [30] in terms of the RMSE index to forecast 1h ahead. Please note that

**TABLE 22.** RMSE for wind power series prediction by ENF-ADBEL, BPNN, ELMAN, LSTM, VMD-BPNN, VMD-ELMAN, VMD-LSTM, and VMD-K-means-LSTM models.

Time Series	Prediction Network	RMSE
Max Wind Power	ENF-ADBEL	29.75
	BP [30]	171.78
	ELMAN [30]	207.71
	LSTM [30]	156.01
	VMD-BPNN [30]	339.6
	VMD-ELMAN [30]	280.55
	VMD-LSTM [30]	151.95
	VMD-Kmeans-LSTM [30]	136.6

the proposed ENF-ADBEL was deployed for different wind power series and that no prior training was required, making the proposed ENF-ADBEL a perfect candidate for online prediction.

**TABLE 23.** RMSE &  $R^2$  for max wind power prediction by ENF-ADBEL and MLP networks.

Time Series	Prediction Network	RMSE	$R^2$ (%)	PI(%)
Max Wind Power	ENF-ADBEL	29.75	99.78	25.13
	MLP	39.74	99.25	

We applied the an MLP neural network for the same wind power data (max power) to validate the proposed ENF-ADBEL. The comparison results given in Table 23 clearly show that the ENF-ADBEL network performed with better accuracy.

- 1) **Highlight 1:** In the proposed ENF-ADBEL model, neo-fuzzy neurons are applied in the orbitofrontal cortex section and partially in the amygdala section of the adaptive decayed brain emotional learning network. Partial integration is done purposefully, as the amygdala section has two outputs: the one that relies on the imprecise information is set free from neo-fuzzy integration to keep the limbic system’s computational principle.
- 2) **Highlight 2:** The integration of the neo-fuzzy network in the amygdala section does not increase the resulting proposed model’s computational complexity to a noticeable extent.
- 3) **Highlight 3:** The Learning parameters, named  $\alpha$ ,  $\beta$ , and  $\gamma$ , play a crucial role in the proposed ENF- ADBEL performance. Currently, an exhaustive search is done to find the near-optimal parameters.
- 4) **Highlight 4:** The proposed ENF-ADBEL model has no prior knowledge of the time-series data, implying that no prior training is required.
- 5) **Highlight 5:** A comparison of the proposed predictor with F-ADBEL [3], NF-ADBEL [2] and others reveals its superiority for time series prediction problems with shorter update intervals.
- 6) **Highlight 6:** It is known that the size of data can affect the performance of predictors. The proposed model can also be deployed where the size of the data is considerably large.

#### IV. CONCLUSION

This paper presented a novel design for a hybrid model of a neo-fuzzy adaptive decayed brain emotional learning network, intending to enhance the prediction accuracy of NF-ADBEL for online time series prediction. The resulting prediction network is called the expanded neo-fuzzy adaptive decayed brain emotional learning (ENF-ADBEL) network. The proposed model was developed by integrating the neo-fuzzy neurons in the orbitofrontal cortex (OFC) section and partially implemented in the amygdala (AMY) section. The proposed model combines competitive emotional neural networks with neo-fuzzy neurons to yield an effective ENF-ADBEL predictor that offers features such as low computational complexity and fast learning. Low complexity is obtained as a result of fewer membership functions being used in neo-fuzzy neuron networks, while fast learning is inherited by employing the emotion-processing mechanism of the mammalian brain.

The proposed ENF-ADBEL network is implemented in a MATLAB programming environment and deployed to predict a selection of chaotic time series classes, including Mackey-Glass, Lorenz, Rossler and the disturbance storm time index. Simulations were conducted to identify a dynamic Narendra plant model and stochastic problems, namely, wind speed and wind power series. To keep the computational complexity at a minimum, we only used three neo-fuzzy neurons membership functions for processing each feature in all OFC and AMY sections of ENF-ADBEL. The proposed model enhanced the prediction accuracy of online time series prediction with no prior training.

The performance of the model was also evaluated in terms of RMSE and  $R^2$ . To draw a comparison, the NF-ADBEL and F-ADBEL networks were simulated as well to forecast the same time series with near-optimal parameters, and the MLP network was applied to draw a comparison to the proposed model. Furthermore, a comparison of the proposed ENF-ADBEL with other used methods in state-of-the-art was made, and a percentage improvement index was defined to compare the proposed model’s performance with the NF-ADBEL and F-ADBEL networks.

Comparing the proposed ENF-ADBEL model with some state-of-the-art predictors reveals its superior performance. The model offers low RMSE and high  $R^2$ . A fair amount of percentage improvement in wind speed and wind power forecasting was obtained along with significant improvement in accuracy for online time series prediction. Finally, the simulation results demonstrate that ENF-ADBEL gave the best performance.

Future work could involve neo-fuzzy neuron implementation in the thalamus and sensory cortex sections to further investigate and test the ENF-ADBEL network’s performance.

#### REFERENCES

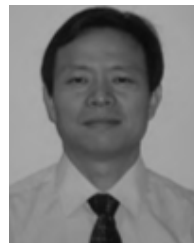
[1] E. Lotfi and M.-R. Akbarzadeh-T, “Adaptive brain emotional decayed learning for online prediction of geomagnetic activity indices,” *Neurocomputing*, vol. 126, pp. 188–196, Feb. 2014.



- [2] H. S. A. Milad, U. Farooq, M. E. El-Hawary, and M. U. Asad, "Neo-fuzzy integrated adaptive decayed brain emotional learning network for online time series prediction," *IEEE Access*, vol. 5, pp. 1037–1049, 2017.
- [3] H. S. A. Milad, U. Farooq, M. E. El-Hawary, V. E. Balas, and M. U. Asad, "Fuzzy logic based parameter adjustment model for adaptive decayed brain emotional learning network with application to online time series prediction," in *Proc. IEEE Electr. Power Energy Conf. (EPEC)*, Oct. 2017, pp. 1–6.
- [4] B. Ferry, B. Roozendaal, and J. L. McGaugh, "Role of norepinephrine in mediating stress hormone regulation of long-term memory storage: A critical involvement of the amygdala," *Biol. Psychiatry*, vol. 46, no. 9, pp. 1140–1152, Nov. 1999.
- [5] E. Kandel, J. Schwartz, and T. Jessell, *Principles of Neural Science*, 4th ed. New York, NY, USA: McGraw-Hill, 2000.
- [6] C. Balkenius and J. Morán, "Emotional learning: A computational model of the amygdala," *Cybern. Syst.*, vol. 32, no. 6, pp. 611–636, Sep. 2001.
- [7] A. Gholipour, C. Lucas, and D. Shahmirzadi, "Purposeful prediction of space weather phenomena by simulated emotional learning," *Int. J. Model. Simul.*, vol. 24, no. 2, pp. 65–72, Jan. 2004.
- [8] M. U. Asad, U. Farooq, J. Gu, J. Amin, A. Sadaqat, M. E. El-Hawary, and J. Luo, "Neo-fuzzy supported brain emotional learning based pattern recognizer for classification problems," *IEEE Access*, vol. 5, pp. 6951–6968, 2017.
- [9] U. Farooq, J. Gu, V. Balas, G. Abbas, M. U. Asad, and M. Balas, "A hybrid time series forecasting model for disturbance storm time index using a competitive brain emotional neural network and neo-fuzzy neurons," *Acta Polytechnica Hungarica*, vol. 16, no. 4, pp. 213–219, Jul. 2019.
- [10] K. Ma and H. Leung, "A novel LSTM approach for asynchronous multivariate time series prediction," in *Proc. Int. Joint Conf. Neural Netw. (IJCNN)*, Jul. 2019, pp. 1–7.
- [11] M. Mackey and L. Glass, "Oscillation and chaos in physiological control systems," *Science*, vol. 197, no. 4300, pp. 287–289, Jul. 1977.
- [12] B. B. Ustundag and A. Kulaglic, "High-performance time series prediction with predictive error compensated wavelet neural networks," *IEEE Access*, vol. 8, pp. 210532–210541, 2020.
- [13] D. Zhang and M. Jiang, "Hetero-dimensional multitask neuroevolution for chaotic time series prediction," *IEEE Access*, vol. 8, pp. 123135–123150, 2020.
- [14] H. Menghui and L. Yian, "Short-term prediction of BP neural network based on difference method," in *Proc. 19th Int. Symp. Distrib. Comput. Appl. Bus. Eng. Sci. (DCABES)*, Oct. 2020, pp. 58–61.
- [15] D. Huang, C. Zhang, Q. Li, H. Han, D. Huang, T. Li, and C. Wang, "Prediction of solar photovoltaic power generation based on MLP and LSTM neural networks," in *Proc. IEEE 4th Conf. Energy Internet Energy Syst. Integr. (EI2)*, Oct. 2020, pp. 2744–2748.
- [16] E. N. Lorenz, "Deterministic nonperiodic flow," *J. Atmos. Sci.*, vol. 20, no. 2, pp. 130–148, Mar. 1963.
- [17] M. Han, S. Zhang, M. Xu, T. Qiu, and N. Wang, "Multivariate chaotic time series online prediction based on improved kernel recursive least squares algorithm," *IEEE Trans. Cybern.*, vol. 49, no. 4, pp. 1160–1172, Apr. 2019.
- [18] Y. Liu, Y. Xu, J. Yang, and S. Jiang, "A polarized random Fourier feature kernel least-mean-square algorithm," *IEEE Access*, vol. 7, pp. 50833–50838, 2019.
- [19] Q. Luo, X. Fang, Y. Sun, J. Ai, and C. Yang, "Self-learning hot data prediction: Where echo state network meets NAND flash memories," *IEEE Trans. Circuits Syst. I, Reg. Papers*, vol. 67, no. 3, pp. 939–950, Mar. 2020.
- [20] S. Shao and X. Gao, "Synchronization in time-delayed fractional order chaotic Rossler systems," in *Proc. Int. Conf. Commun., Circuits Syst.*, May 2008, pp. 652–654.
- [21] WDC. (2000). *Geomagnetic Equatorial DST Index Home Page*. [Online]. Available: [http://wdc.kugi.kyoto-u.ac.jp/dst\\_final/200004/index.html](http://wdc.kugi.kyoto-u.ac.jp/dst_final/200004/index.html)
- [22] A. U. Haque, P. Mandal, J. Meng, M. E. Kaye, and L. Chang, "A new strategy for wind speed forecasting using hybrid intelligent models," in *Proc. 25th IEEE Can. Conf. Electr. Comput. Eng. (CCECE)*, Apr. 2012, pp. 1–4.
- [23] L. Lazić, G. Pejanović, and M. Živković, "Wind forecasts for wind power generation using the eta model," *Renew. Energy*, vol. 35, no. 6, pp. 1236–1243, Jun. 2010.
- [24] M. Negnevitsky, P. Johnson, and S. Santoso, "Short term wind power forecasting using hybrid intelligent systems," in *Proc. IEEE Power Eng. Soc. Gen. Meeting*, Jun. 2007, pp. 1–4.
- [25] (2020). *Climate Data Hourly Data*. [Online]. Available: [https://climate.weather.gc.ca/climate\\_data/hourly\\_data\\_e.html#range=2002-07-12T2021-01-12&dlyRange=2005-11-01T2021-01-1&mlyRange=2007-07-01T2007-07-01&StationID=31829&Prov=NS&urlExtension=\\_e.html&searchType=stnProv&optLimit=yearRange&StartYear=2020&EndYear=2021&selRowPerPage=25&Line=24&Month=1&Month=2&Month=3&1stProvince=NS&timeframe=1&Year=2020](https://climate.weather.gc.ca/climate_data/hourly_data_e.html#range=2002-07-12T2021-01-12&dlyRange=2005-11-01T2021-01-1&mlyRange=2007-07-01T2007-07-01&StationID=31829&Prov=NS&urlExtension=_e.html&searchType=stnProv&optLimit=yearRange&StartYear=2020&EndYear=2021&selRowPerPage=25&Line=24&Month=1&Month=2&Month=3&1stProvince=NS&timeframe=1&Year=2020)
- [26] Y. Long and R. Zhang, "Short-term wind speed prediction with ensemble algorithm," in *Proc. Chin. Autom. Congr. (CAC)*, Nov. 2020, pp. 6192–6196.
- [27] Y.-K. Wu, S.-M. Chang, and P. Mandal, "Grid-connected wind power plants: A survey on the integration requirements in modern grid codes," *IEEE Trans. Ind. Appl.*, vol. 55, no. 6, pp. 5584–5593, Dec. 2019.
- [28] Y. Xue, C. Yu, J. Zhao, K. Li, X. Liu, Q. Wu, and G. Yang, "A review on short-term and ultra-short-term wind power prediction," *Dianli Xitong Zidonghua/Automat. Electr. Power Syst.*, vol. 39, pp. 141–151, Mar. 2015.
- [29] AESO. (2021). *Alberta 12 Hour Wind Power Forecast Updated as of 1/28/2021*. [Online]. Available: <https://www.aeso.ca/grid/forecasting/wind-power-forecasting>
- [30] Z. Sun, S. Zhao, and J. Zhang, "Short-term wind power forecasting on multiple scales using VMD decomposition, K-means clustering and LSTM principal computing," *IEEE Access*, vol. 7, pp. 166917–166929, 2019.



**HOUSSEIN SALH ALI MILAD** (Member, IEEE) received the B.Sc. degree (Hons.) in electrical engineering from Hoon University, Hoon, Libya, in 1992, and the M.A.Sc. degree in electrical and computer engineering (power systems) from Dalhousie University, Halifax, NS, Canada, in 2008, where he is currently pursuing the Ph.D. degree. His research interests include forecasting, modeling, and control of power systems.



**JASON GU** (Senior Member, IEEE) received the bachelor's degree in electrical engineering and information science from the University of Science and Technology of China, in 1992, the master's degree in biomedical engineering from Shanghai Jiao Tong University, in 1995, and the Ph.D. degree from the University of Alberta, Canada, in 2001. He is currently a Full Professor of electrical and computer engineering with Dalhousie University, Canada. He is also a Cross-Appointed Professor with the School of Biomedical Engineering for his multidisciplinary research work. He has over 19 years of research and teaching experience and has authored over 260 conference papers and articles. His research interests include robotics, biomedical engineering, rehabilitation engineering, neural networks, and control. He is a Fellow of the Engineering Institute of Canada. He has been an Associate Editor of the *Journal of Control and Intelligent Systems*, *Transactions on CSME*, *IEEE TRANSACTION ON MECHATRONICS*, *International Journal of Robotics and Automation*, *Unmanned Systems*, *Journal of Engineering and Emerging Technologies*, and *IEEE ACCESS*.

• • •